

YneA, an SOS-Induced Inhibitor of Cell Division in *Bacillus subtilis*, Is Regulated Posttranslationally and Requires the Transmembrane Region for Activity^{∇†}

Allison H. Mo and William F. Burkholder*

Department of Biology, Stanford University, Stanford, California 94305-5020

Received 12 January 2010/Accepted 23 March 2010

Cell viability depends on the stable transmission of genetic information to each successive generation. Therefore, in the event of intrinsic or extrinsic DNA damage, it is important that cell division be delayed until DNA repair has been completed. In *Bacillus subtilis*, this is accomplished in part by YneA, an inhibitor of division that is induced as part of the SOS response. We sought to gain insight into the mechanism by which YneA blocks cell division and the processes involved in shutting off YneA activity. Our data suggest that YneA is able to inhibit daughter cell separation as well as septum formation. YneA contains a LysM peptidoglycan binding domain and is predicted to be exported. We established that the YneA signal peptide is rapidly cleaved, resulting in secretion of YneA into the medium. Mutations within YneA affect both the rate of signal sequence cleavage and the activity of YneA. YneA does not stably associate with the cell wall and is rapidly degraded by extracellular proteases. Based on these results, we hypothesize that exported YneA is active prior to signal peptide cleavage and that proteolysis contributes to the inactivation of YneA. Finally, we identified mutations in the transmembrane segment of YneA that abolish the ability of YneA to inhibit cell division, while having little or no effect on YneA export or stability. These data suggest that protein-protein interactions mediated by the transmembrane region may be required for YneA activity.

As cells grow and divide, their survival is dependent on the stable transmission of genetic information to each successive generation. This requires that chromosomes be accurately duplicated and segregated, and in the event of intrinsic or extrinsic DNA damage, that they be accurately repaired. One way that bacteria are able to sense DNA stress and react accordingly is through the widely conserved SOS response (reviewed in references 22, 33, 34, and 48). The SOS response is initiated when single-stranded DNA accumulates following DNA damage or replication blocks. Two proteins, RecA and LexA, regulate the SOS response: RecA recognizes and forms filaments on single-stranded DNA, promoting the autocleavage of LexA, a DNA-binding protein that represses transcription of genes in the SOS regulon (2, 38, 39, 52). Subsequent transcription of these SOS genes activates processes such as excision repair, translesion synthesis, and homologous recombination, as well as inhibition of cell division (2, 22, 34, 36, 52).

In *Escherichia coli*, the gene responsible for the inhibition of cell division during the SOS response, *sfiA* (or *sulA*), has been well characterized (31, 32; reviewed in references 3 and 10). SfiA blocks polymerization of FtsZ, a tubulin orthologue that forms a ring at mid-cell and constitutes an early step of division (15, 30, 57). In addition, SfiA is rapidly degraded by the Lon protease (43), allowing cells to quickly resume dividing once chromosome perturbations have been repaired.

Bacillus subtilis has a functional counterpart of *sfiA*, *yneA*, which is transcribed divergently from *lexA* (35). Like SfiA, YneA inhibits cell division as part of the SOS response (35). As with other genes in the SOS regulon, *yneA* expression is repressed by LexA. DNA-damaging agents such as mitomycin C, which creates interstrand DNA cross-links, induce the SOS response and result in *yneA*-dependent cell elongation (35). Overexpression of *yneA* also leads to elongated cell morphology, reflecting the continuation of cell growth in the absence of division (35).

Despite similarities in function, YneA and SfiA likely act by different mechanisms. YneA differs greatly from SfiA in sequence and predicted secondary structure. Whereas SfiA is a cytosolic protein, YneA is predicted to be a secreted protein with a short cytoplasmic N-terminal sequence and a single-pass transmembrane domain followed by a putative signal peptide cleavage site. The extracellular portion of YneA contains a single LysM peptidoglycan binding domain and a short C-terminal sequence. Many proteins that contain one or more LysM domains, including some autolysins, are involved in peptidoglycan remodeling, a process that is important for septum formation and daughter cell separation (4, 13, 61). It is unknown what role, if any, the LysM domain in YneA plays in blocking cell division. YneA and SfiA also differ in their interactions with FtsZ. While SfiA binds directly to and inhibits FtsZ in the cytoplasm, two-hybrid analysis does not detect any interaction between YneA and FtsZ (35). FtsZ ring formation is merely reduced, not abolished, in *yneA*-overexpressing cells, possibly as an indirect result of YneA activity (35).

Recently, SOS-inducible inhibitors of cell division have been characterized in other Gram-positive bacteria, including *Listeria monocytogenes* YneA (58, 59), *Mycobacterium tuberculosis* Rv2719c (11, 14), and *Corynebacterium glutamicum* DivS (45).

* Corresponding author. Mailing address: Department of Biology, Stanford University, 371 Serra Mall, Stanford, CA 94305-5020. Phone: (650) 724-1504. Fax: (650) 723-0155. E-mail: burkholder@stanford.edu.

† Supplemental material for this article may be found at <http://j.b.asm.org/>.

∇ Published ahead of print on 16 April 2010.

Rv2719c interferes with FtsZ ring formation, localizes to sites of nascent peptidoglycan synthesis, and displays cell wall hydrolase activity (14). Rv2719c has a large N-terminal region facing the interior of the cell that is not present in YneA. This N-terminal portion, together with the transmembrane segment, is sufficient for both hydrolase activity and inhibition of division. Rv2719c also has a single extracellular LysM domain that does not appear to be necessary for function (14). However, given the differences in structure between Rv2719c and YneA, it is unclear whether the LysM domain in YneA is similarly dispensable.

C. glutamicum DivS lacks a LysM domain and does not have significant sequence homology to either Rv2719c or YneA. *divS* overexpression reduces the number of FtsZ rings, yet as was the case for YneA, DivS does not appear to interact directly with FtsZ (45). Zones of nascent peptidoglycan synthesis are reduced in mitomycin C-treated *C. glutamicum* cells, suggesting that DivS interferes with septal wall synthesis. Interestingly, the N terminus of DivS appears to be dispensable for function, whereas the extracellular C terminus is required for activity (45). This is the opposite of what is seen with Rv2719c.

Given the diverse structures and proposed mechanisms of the SOS-induced cell division inhibitors that have been characterized so far, we set out to further investigate the effect of YneA on cell division. Here we show that YneA delays daughter cell separation in addition to septum formation. Our biochemical analysis indicates that YneA is rapidly cleaved and exported via the SecA pathway and that association with the cell wall is transient. Surprisingly, it appears that YneA is active in its full-length form, prior to signal peptide cleavage. Lastly, the transmembrane domain of YneA is required for function, independent of its role in protein export, perhaps due to critical intramembrane protein interactions. This suggests that YneA interacts with an unidentified transmembrane target to transiently delay cell division, after which YneA is rapidly cleaved and released from the membrane. Thus, YneA has a unique and finely tuned mechanism allowing swift resumption of the cell cycle once DNA damage has been repaired and the SOS response is shut off.

MATERIALS AND METHODS

Media. Strains were grown in LB medium (42), CH and SM media (27), germination (GMD) medium (26), or GYE medium (47). CH, SM, and GYE media were supplemented with required amino acids (40 $\mu\text{g ml}^{-1}$). GYE indicator plates for PhoA assays contained 50 $\mu\text{g ml}^{-1}$ XP (5-bromo-4-chloro-3-indolylphosphate, *p*-toluidine salt; Sigma). Competent cells were prepared essentially as described by Msadek et al. (44), replacing GE medium with MD medium (100 mM potassium phosphate, pH 7.5, 4 mM trisodium citrate, 2% [wt/vol] glucose, 11 mg liter⁻¹ ferric ammonium citrate, 0.25% [wt/vol] potassium aspartate, 3 mM MgSO₄, 50 $\mu\text{g ml}^{-1}$ L-tryptophan, and 50 $\mu\text{g ml}^{-1}$ L-phenylalanine). Antibiotic resistance markers were selected using the following drug concentrations: for *amp*, 100 $\mu\text{g ml}^{-1}$ ampicillin; for *cat*, 5 $\mu\text{g ml}^{-1}$ chloramphenicol; for *erm*, 0.5 $\mu\text{g ml}^{-1}$ erythromycin and 12.5 $\mu\text{g ml}^{-1}$ lincomycin; for *kan*, 5 $\mu\text{g ml}^{-1}$ kanamycin; and for *spc*, 100 $\mu\text{g ml}^{-1}$ spectinomycin.

Plasmids and strains. Strains used in this study are listed in Table 1, and plasmids and oligonucleotides used in this study are listed in Tables S1 and S2 in the supplemental material. Strains used in the experiments are derivatives of strain JH642 and have the common genotype *trpC2 pheA1* (9), unless otherwise noted. See the supplemental material for details on the construction of strains and plasmids.

The FtsZ-yellow fluorescent protein (FtsZ-YFP) fusion in strain AM293 has been described previously (21). Genomic DNA from strain 1058

[*amyE::*(P_{spn}^{ank(hy)}*ftsZ-yfp spc*); kindly provided by Peter Lewis] was used to generate strains in the JH642 strain background. Strain AM280 was derived from the temperature-sensitive *secA* mutant TB301 [*B. subtilis* strain 168 *secA341*(Ts) *trpC2*] (kindly provided by Kunio Yamane [28]). Strain AM200 was derived from extracellular protease mutant WE1 (*B. subtilis* strain 168 *epi::tet wrpA::kan trpC2*) (kindly provided by Junichi Sekiguchi [61]).

Overexpression of yneA. Unless indicated otherwise in the figures, strains containing P_{spn}^{ank(hy)}*yneA*, P_{spn}^{ank(hy)}*yneA-phoA*, and P_{spn}^{ank(hy)}*yneA-S-flag-his10* were grown overnight in liquid LB cultures, diluted to an optical density at 600 nm (OD₆₀₀) of ~0.02 in LB medium, and incubated at 37°C. In experiments involving *phoA*-tagged strains, GYE minimal medium, in which endogenous *phoA* expression is repressed, was used instead of LB medium. Upon reaching exponential phase (OD₆₀₀ = 0.3 to 0.5), *yneA* (or its epitope-tagged forms) was induced with 1 mM IPTG (isopropyl- β -D-thiogalactopyranoside).

Microscopy. Samples were taken for fluorescence microscopy (0.5 to 1.0 ml) at the times indicated in the figures. Cells were pelleted by centrifugation for 1 min at 5,000 \times g and were resuspended in a small amount (~50 μl) of 1 \times phosphate-buffered saline (PBS). Cell membranes were visualized using the fluorescent dye FM4-64 (10 $\mu\text{g ml}^{-1}$ [final concentration]; Invitrogen), and DNA was visualized using DAPI (4',6-diamidino-2-phenylindole; 2 $\mu\text{g ml}^{-1}$). Samples were immobilized on either 1% agarose pads or coverslips treated with 0.1% poly-L-lysine solution (Sigma) and were visualized using a Zeiss AxioImager M1 microscope fitted with an Orca-ER charge-coupled device (CCD) camera (Hamamatsu). The following Zeiss filter sets were used: 43 (FM4-64), 46 (YFP), and 49 (DAPI). Images were collected and processed using Openlab 5 (Improvision).

Spore preparation and germination. Spores were prepared as described previously (26). Briefly, cells were spread on potato dextrose agar plates and incubated for several days to obtain spores. The spores were washed twice with water, resuspended in Tris-EDTA (TE) buffer, treated with 1 mg ml⁻¹ lysozyme (Sigma) for 1 h at 37°C, and shaken with 2% sodium dodecyl sulfate (SDS) for 45 min. Spores were then repeatedly washed with sterile distilled water (with pelleting of spores by centrifugation at 4,000 \times g for 10 min) until the supernatant remained clear. Spore preparations were inspected by microscopy to ensure that phase-bright spores comprised at least 90% of visible particles. Spores were stored in sterile distilled water at 4°C.

Potato dextrose agar plates were prepared as follows (protocol kindly provided by Liz Harry, University of Technology, Sydney, Australia). Potato dextrose agar (35.6 g; Difco) and 15 g Bacto agar (Difco) were added to 1.25 liters deionized water and autoclaved. After cooling of the agar to 50°C, the following supplements were added and the final volume was adjusted to 1.5 liters (amounts given are final concentrations): 1 \times Spizizen's minimal salts [125 mM potassium phosphate (14 g liter⁻¹ K₂HPO₄, 6 g liter⁻¹ KH₂PO₄), 15 mM (NH₄)₂SO₄, 3.4 mM sodium citrate, 0.8 mM MgSO₄], 20 μM MnCl₂, 360 μM CaCl₂, 1 \times trace elements solution containing (per liter) 125 mg MgCl₂ · 6H₂O, 5.5 mg CaCl₂, 13.5 mg FeCl₂ · 6H₂O, 1.0 mg MnCl₂ · 4H₂O, 1.7 mg ZnCl₂, 0.43 mg CuCl₂ · 2H₂O, 0.6 mg CoCl₂ · 6H₂O, and 0.6 mg Na₂MoO₄ · 2H₂O (27), 40 $\mu\text{g ml}^{-1}$ tryptophan, and 40 $\mu\text{g ml}^{-1}$ phenylalanine.

To germinate spores, purified spores were resuspended in 10 ml sterile deionized water to a final OD₆₀₀ of 1. Spores were incubated at 80°C for 30 min and then allowed to cool for 10 min at room temperature. The spores were centrifuged at 3,500 \times g for 10 min, resuspended in an equal volume of prewarmed GMD medium, and incubated at 37°C with shaking (the 0-min time point). IPTG (1 mM [final concentration]) was added at the time of resuspension to induce *yneA*. Samples were collected at the indicated times and visualized by fluorescence microscopy.

Cell fractionation. Strains were grown overnight in LB medium and then diluted to a final OD₆₀₀ of 0.02 to 0.04 in 20 ml GYE medium. Cells were grown at 37°C, and *yneA-phoA* expression was induced with IPTG (1 mM [final concentration]) for 2 h. To separate the cell and secreted fractions, the cultures were centrifuged at 3,500 \times g for 10 min, and the supernatant was concentrated to 1/10 the original volume (~1.6 ml), using Amicon Ultra-15 centrifugal filter units (30 kDa; Millipore); YneA-PhoA is 58.6 kDa. Proteins bound to the cell wall (wall fraction) were extracted from the cell fraction by use of high concentrations of LiCl as described previously (61). Briefly, the cell pellet was washed twice with 20 mM Tris-Cl (pH 7.5), resuspended in 400 μl LiCl solution (20 mM Tris-Cl, pH 7.5, 3 M LiCl), and incubated on ice for 15 min. Samples were centrifuged at 5,000 \times g for 10 min, and supernatant containing cell wall-bound proteins was removed to a fresh tube on ice. The cell pellet was washed once with lysis buffer (50 mM Tris-Cl, pH 7.5, 50 mM NaCl, 5 mM MgCl₂), resuspended in 50 to 200 μl lysis buffer containing lysozyme and detergent (50 mM Tris-Cl, pH 7.5, 50 mM NaCl, 5 mM MgCl₂, 0.5 mg ml⁻¹ lysozyme, 0.2% Triton X-100, 100 U ml⁻¹ DNase I, 20 $\mu\text{g ml}^{-1}$ RNase A, 0.5% [vol/vol] protease inhibitor cocktail [Sigma P-8849]), and incubated at 37°C for 10 min. The lysate was centrifuged at

TABLE 1. Strains used in this study

Strain	Genotype	Reference
AM62	<i>amyE::pDG1662 (cat) trpC2 pheA1</i>	
AM69	<i>amyE::pAM45 [spc P_{spank(hy)}-yneA lacI] trpC2 pheA1</i>	
AM70	<i>amyE::pDR111 [spc P_{spank(hy)} lacI] trpC2 pheA1</i>	
AM93	<i>amyE::pAM67 [cat P_{spank(hy)}-yneA lacI] trpC2 pheA1</i>	
AM98	<i>thrC::pAM73 [erm P_{spank(hy)}-yneA-phoA lacI] trpC2 pheA1</i>	
AM133	<i>amyE::pAM89 [spc P_{spank(hy)}-yneA(ASAA) lacI] trpC2 pheA1</i>	
AM155	<i>amyE::pAM115 [spc P_{spank(hy)}-yneA(D97A) lacI] trpC2 pheA1</i>	
AM175	<i>amyE::pAM129 [spc P_{spank(hy)}-yneA(E6A) lacI] trpC2 pheA1</i>	
AM187	<i>thrC::pAM133 [erm P_{spank(hy)}-yneA(E6A)-phoA lacI] trpC2 pheA1</i>	
AM199	<i>thrC::pAM148 [erm P_{spank(hy)}-yneA-S-flag-his10 lacI] trpC2 pheA1</i>	
AM200	<i>thrC::pAM148 [erm P_{spank(hy)}-yneA-S-flag-his10 lacI] epr::tet wprA::kan trpC2</i>	
AM202	<i>thrC::pAM150 [erm P_{spank(hy)}-yneA(ASAA)-S-flag-his10 lacI] trpC2 pheA1</i>	
AM206	<i>thrC::pAM72 [erm P_{spank(hy)} lacI] trpC2 pheA1</i>	
AM214	<i>yneA::pAM157 (erm single crossover; yields . . . yneA-S-flag-his10 erm bla 'yneA . . .) trpC2 pheA1</i>	
AM218	<i>lytE::pAM160 (cat single crossover; yields . . . lytE-phoA cat bla 'lytE . . .) trpC2 pheA1</i>	
AM220	<i>amyE::pAM162 [spc P_{spank(hy)}-yneA(L25A) lacI] trpC2 pheA1</i>	
AM221	<i>amyE::pAM163 [spc P_{spank(hy)}-yneA(S26A) lacI] trpC2 pheA1</i>	
AM222	<i>lytE::pAM160 (cat single crossover; yields . . . lytE-phoA cat bla 'lytE . . .) thrC::pAM73[erm P_{spank(hy)}-yneA-phoA lacI] trpC2 pheA1</i>	
AM228	<i>thrC::pAM166 [erm P_{spank(hy)}-yneA(D97A)-S-flag-his10 lacI] trpC2 pheA1</i>	
AM232	<i>amyE::pAM169 [spc P_{spank(hy)}-yneA(S7A) lacI] trpC2 pheA1</i>	
AM233	<i>amyE::pAM170 [spc P_{spank(hy)}-yneA(I8A) lacI] trpC2 pheA1</i>	
AM234	<i>amyE::pAM171 [spc P_{spank(hy)}-yneA(I9A) lacI] trpC2 pheA1</i>	
AM235	<i>amyE::pAM172 [spc P_{spank(hy)}-yneA(F10A) lacI] trpC2 pheA1</i>	
AM236	<i>amyE::pAM173 [spc P_{spank(hy)}-yneA(V11A) lacI] trpC2 pheA1</i>	
AM237	<i>amyE::pAM174 [spc P_{spank(hy)}-yneA(L13A) lacI] trpC2 pheA1</i>	
AM238	<i>amyE::pAM175 [spc P_{spank(hy)}-yneA(F14A) lacI] trpC2 pheA1</i>	
AM239	<i>amyE::pAM176 [spc P_{spank(hy)}-yneA(T15A) lacI] trpC2 pheA1</i>	
AM240	<i>amyE::pAM177 [spc P_{spank(hy)}-yneA(V16A) lacI] trpC2 pheA1</i>	
AM241	<i>amyE::pAM178 [spc P_{spank(hy)}-yneA(I17A) lacI] trpC2 pheA1</i>	
AM242	<i>amyE::pAM180 [spc P_{spank(hy)}-yneA(S19A) lacI] trpC2 pheA1</i>	
AM243	<i>amyE::pAM181 [spc P_{spank(hy)}-yneA(V21A) lacI] trpC2 pheA1</i>	
AM244	<i>amyE::pAM182 [spc P_{spank(hy)}-yneA(I22A) lacI] trpC2 pheA1</i>	
AM245	<i>amyE::pAM183 [spc P_{spank(hy)}-yneA(L23A) lacI] trpC2 pheA1</i>	
AM247	<i>thrC::pAM185 [erm P_{spank(hy)}-yneA(S7A)-phoA lacI] trpC2 pheA1</i>	
AM248	<i>thrC::pAM186 [erm P_{spank(hy)}-yneA(I8A)-phoA lacI] trpC2 pheA1</i>	
AM250	<i>thrC::pAM188 [erm P_{spank(hy)}-yneA(F10A)-phoA lacI] trpC2 pheA1</i>	
AM252	<i>thrC::pAM190 [erm P_{spank(hy)}-yneA(L13A)-phoA lacI] trpC2 pheA1</i>	
AM253	<i>thrC::pAM191 [erm P_{spank(hy)}-yneA(F14A)-phoA lacI] trpC2 pheA1</i>	
AM254	<i>thrC::pAM192 [erm P_{spank(hy)}-yneA(T15A)-phoA lacI] trpC2 pheA1</i>	
AM255	<i>thrC::pAM193 [erm P_{spank(hy)}-yneA(I17A)-phoA lacI] trpC2 pheA1</i>	
AM256	<i>thrC::pAM194 [erm P_{spank(hy)}-yneA(S19A)-phoA lacI] trpC2 pheA1</i>	
AM257	<i>thrC::pAM195 [erm P_{spank(hy)}-yneA(V21A)-phoA lacI] trpC2 pheA1</i>	
AM258	<i>thrC::pAM196 [erm P_{spank(hy)}-yneA(I22A)-phoA lacI] trpC2 pheA1</i>	
AM259	<i>thrC::pAM197 [erm P_{spank(hy)}-yneA(L23A)-phoA lacI] trpC2 pheA1</i>	
AM260	<i>thrC::pAM184 [erm P_{spank(hy)}-yneA(L25A)-phoA lacI] trpC2 pheA1</i>	
AM261	<i>thrC::pAM199 [erm P_{spank(hy)}-yneA(T15A)-S-flag-his10 lacI] trpC2 pheA1</i>	
AM263	<i>thrC::pAM200 [erm P_{spank(hy)}-yneA(V21A)-S-flag-his10 lacI] trpC2 pheA1</i>	
AM280	<i>secA314(Ts) thrC::pAM73 [erm P_{spank(hy)}-yneA-phoA lacI] trpC2</i>	
AM293	<i>amyE::spc P_{xy1}-ftsZ-yfp thrC::pAM224 [erm P_{spank(hy)}-yneA lacI] trpC2 pheA1</i>	
JH642	<i>trpC2 pheA1</i>	9
SB881	<i>amyE::spc P_{xy1}-ftsZ-yfp trpC2 pheA1</i>	S. J. Biller, unpublished lab strain
TB301	<i>secA314(Ts) trpC2</i>	28
WE1	<i>epr::tet wprA::kan trpC2</i>	61

16,000 × g for 2 min to remove debris, and the supernatants were transferred to fresh tubes on ice.

Proteins in the cell wall and secreted fractions were precipitated with trichloroacetic acid (TCA) and resuspended in 50 µl urea lysis buffer (100 mM NaH₂PO₄, 10 mM Tris-Cl, pH 8.0, 8 M urea). Protein concentrations of all fractionated samples were determined by Bradford assay (Bio-Rad).

For separation of cell fractions in experiments with strains carrying the *secA314(Ts)* mutation (see Fig. 5C), strains were grown in GYE medium as described above, but at 30°C instead of 37°C. Upon reaching exponential phase (OD₆₀₀ = 0.3), cells were washed once with T-base, resuspended in GYE medium containing 1 mM IPTG, and incubated at either 30°C or 45°C. After 1 h of

induction, cultures were centrifuged and the secreted fraction prepared as described above. The cell pellet was washed once with Tris-Cl (pH 7.5) and then treated with lysozyme and detergent as described above, but omitting the treatment with LiCl (leaving wall-associated proteins in the cell fraction). Protein concentrations were measured by Bradford assay.

Proteolysis rate experiments. Experiments to determine rates of proteolysis were adapted from previously described methods (49). Strains were grown and S protein-tagged YneA fusions were induced with IPTG (final concentration, 1 mM) as described in the figure legends. After 1 h of induction, protein synthesis was arrested by adding chloramphenicol to a final concentration of 200 µg ml⁻¹, and a 1-ml sample was immediately removed to a tube containing trichloroacetic

acid (final concentration, 10% [wt/vol]) and incubated on ice (0-min time point). In the same manner, additional 1-ml samples were removed at the time points indicated in the figures. Cell material and proteins were centrifuged, washed with acetone, and air dried. The pellet was resuspended in 500 μ l immunoprecipitation (IP) lysis buffer (50 mM Tris-Cl, pH 7.8, 10% [wt/vol] sucrose, 5 mM EDTA, 5 μ g ml⁻¹ lysozyme, 0.5% [vol/vol] protease inhibitor cocktail [Sigma P-8849]) and incubated at 37°C for 30 min. Five hundred microliters of IP buffer (100 mM Tris-Cl, pH 7.8, 300 mM NaCl, 1% Triton X-100, 10 mM EDTA, 0.5% [vol/vol] protease inhibitor cocktail [Sigma P-8849]) was then added, and samples were incubated on ice for 30 min. Sample supernatant was collected after centrifugation (16,000 \times g, 2 min).

S protein agarose beads (EMD) were prepared by four washes in IP buffer, with centrifugation at 2,000 \times g for 5 s each time. Supernatants from the centrifuged TCA-precipitated and lysed samples described above were added to 50 μ l of washed beads and incubated overnight on a rotator at 4°C. The S-tagged protein-bound beads were then washed four times with 250 μ l IP wash buffer (50 mM Tris-Cl, pH 7.8, 300 mM NaCl, 0.1% Triton X-100, 5 mM EDTA) and once with 1 ml phosphate-buffered saline, with centrifugation at 2,000 \times g for 5 s each time. After the final wash, all supernatant was removed and the beads were mixed with 10 μ l of phosphate-buffered saline and 4 μ l of 5 \times Laemmli SDS loading buffer. Samples were then incubated at 95°C for 5 min to release the S-tagged protein from the beads. Beads were removed by centrifugation at 16,000 \times g for 2 min, and supernatant was transferred to a fresh tube. Eight microliters of supernatant was loaded into each lane of an SDS-Tris-Tricine-polyacrylamide gel for detection (see "Immunoblot analysis").

Immunoblot analysis. Immunoblots were carried out essentially as described previously (49). Samples for immunoblotting were prepared by adding Laemmli SDS loading buffer to a final concentration of 1 \times . In the experiments to determine rates of proteolysis, 2 μ l of additional 5 \times loading buffer was added to each 8- μ l sample, which aided in gel loading. Ten-microliter samples were separated in 10% SDS-Tris-glycine-polyacrylamide (precast; Bio-Rad), 10% SDS-Tris-Tricine-polyacrylamide, or 13.8% SDS-Tris-Tricine-polyacrylamide gels and transferred to polyvinylidene difluoride (PVDF) membranes. For cell fractionation experiments, the amount of total soluble protein loaded into each lane is indicated in the figures. After being blocked, membranes were probed with monoclonal mouse antibodies raised against PhoA (1:10,000 dilution; Sigma) or S protein (1:5,000 dilution; EMD), followed by incubation with a 1:10,000 dilution of rabbit anti-mouse antibodies conjugated to peroxidase (Sigma). Detection was performed by chemiluminescence using the ECL system (Amersham) and by exposure to X-ray film (Amersham Hyperfilm ECL).

Where indicated, the membrane was stripped and reprobed as follows. The membrane was soaked in membrane stripping buffer (25 mM glycine, 1% SDS, pH 2.0) for 1 h, rinsed twice with phosphate-buffered saline, and reblocked. The membrane was then probed with a 1:5,000 dilution of chicken anti-DnaA antibodies, followed by incubation with donkey anti-chicken secondary antibodies conjugated to horseradish peroxidase (1:10,000 dilution; Jackson Immuno-Research). Detection was carried out as described above.

RESULTS

Overexpression of *yneA* delays cell division. In order to study the effects of YneA on cell division, we placed *yneA* under the control of an IPTG-inducible promoter, P_{spank(hy)}, at an ectopic locus, *amyE*. Kawai et al. previously observed that overexpressing *yneA* results in filamentation (35). Consistent with this, overexpressing *yneA* inhibited the formation of single colonies on LB agar containing 1 mM IPTG (Fig. 1A). Cells were also visibly elongated after an hour of induction (approximately two doublings) (Fig. 1B). As shown in Fig. 1C, overexpression of *yneA* resulted in a range of cell lengths, but on average, cells were 2-fold longer than either uninduced cells or vector control cells. This suggests that cells continued to grow when *yneA* was overexpressed but that formation of the division septum was delayed. Cell density measurements indicated that cultures of *yneA*-overexpressing cells displayed similar growth rates to those of uninduced cultures (see Fig. S1 in the supplemental material).

As another measure of YneA's effect on division, we in-

duced *yneA* in a synchronized culture of germinating spores. Three hours after cells were induced to germinate, nearly all vector control and uninduced cells had divided at least once (Fig. 1D). In contrast, fewer than 10% of *yneA*-overexpressing cells had divided in that time frame. Although the *yneA*-overexpressing cells eventually began dividing, they required an additional 45 min for the fraction of divided cells to approach the level of divided cells in the uninduced culture. Thus, although YneA activity does not result in extreme filamentation, as seen with SfiA in *E. coli*, it still has the clear ability to delay cell division.

Overexpression of *yneA* delays FtsZ ring assembly. While it appears that YneA affects septum formation, it is otherwise unclear which stage of division YneA acts upon. Kawai et al. previously observed that FtsZ rings form at a reduced frequency in *yneA*-overexpressing cells compared to those in wild-type cells, leading them to suggest that YneA may act by inhibiting Z ring formation (35). However, the use of phase-contrast rather than membrane-stained images did not allow for the quantitation of FtsZ rings in relation to cell length. Since overexpression of *yneA* resulted in various degrees of cell elongation (Fig. 1C), we wanted to quantitatively determine whether reduced FtsZ ring formation correlated with increased cell length.

In order to examine the relationship between FtsZ rings and cell elongation, we constructed a strain carrying a xylose-inducible FtsZ-YFP fusion at the *amyE* locus, together with an IPTG-inducible *yneA* gene integrated at *thrC*. When expression of FtsZ-YFP was induced with 0.5% xylose, FtsZ-YFP localized to the mid-cell and the cell poles, as expected (Fig. 2A). We noted that FtsZ-YFP localized to septa or poles rather than the mid-cell in a fairly large fraction of the population for both cells overexpressing *yneA* and uninduced control cells. Although this might reflect an effect of the YFP fusion, cell growth and morphology were unaffected by expression of FtsZ-YFP (data not shown).

We measured cell lengths and sorted the cells by 0.5- μ m increments (Fig. 2B, left y axis). Cells overexpressing *yneA* were elongated overall compared to uninduced cells (Fig. 2A and B), consistent with the results in Fig. 1C. We then determined the average number of nonpolar FtsZ rings per cell for each group of cells binned by cell length (Fig. 2B, right y axis). Our results show that FtsZ ring assembly was delayed in *yneA*-overexpressing cells: *yneA*-overexpressing cells that fell between 3.0 and 4.0 μ m were less likely to contain nonpolar FtsZ rings than uninduced cells of the same length (Fig. 2). Among the longer *yneA*-overexpressing cells, there was a positive correlation between cell length and the average number of nonpolar FtsZ rings per cell. The longest *yneA*-overexpressing cells (>5.0 μ m) contained, on average, more than one FtsZ ring. Therefore, while YneA appears to inhibit FtsZ ring assembly to some extent, Z rings still form in the most elongated cells.

Overexpression of *yneA* inhibits cell separation. Cells of *B. subtilis* typically form chains during exponential growth. Around the time when cells cease exponential growth, the increased activity of several autolysins separates sister cells, gradually reducing chains to single cells (6, 23). In the course of our experiments, we observed that many *yneA*-overexpressing cells remained in chains well into stationary phase. This effect was not due to a delay in the onset of stationary phase,

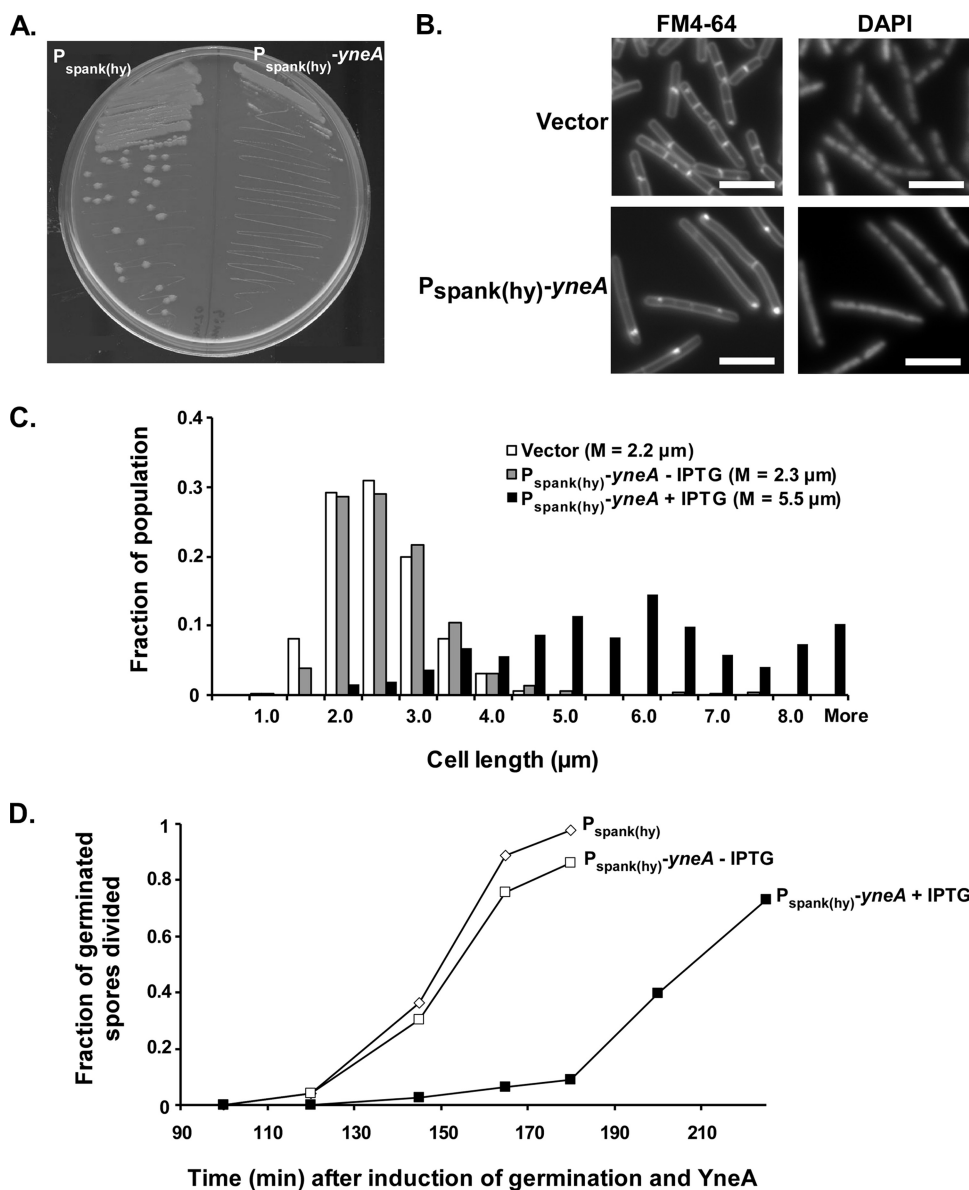


FIG. 1. YneA delays cell division. (A) Strains overexpressing *yneA* are unable to form single colonies on plates. AM69 [*amyE*:: $P_{spank(hy)-yneA}$] and AM70 [*amyE*:: $P_{spank(hy)}$] were streaked onto LB agar containing 1 mM IPTG and grown overnight at 30°C. (B) Cells overexpressing *yneA* are elongated. AM62 [*amyE*::*cat*] and AM93 [*amyE*:: $P_{spank(hy)-yneA}$] were induced with 1 mM IPTG as described in Materials and Methods. One hour after induction, cells were stained with FM4-64 and DAPI and then visualized. Bars, 5 μm . (C) Cell length distributions from the same experiment as that for panel B. At least 300 cells were measured for each strain. The experiment was repeated more than four times under essentially the same conditions. The graph shown here is from a representative experiment. (D) Overexpression of *yneA* delays the first cell division during spore outgrowth. Spore preparations of AM69 [*amyE*:: $P_{spank(hy)-yneA}$] and AM70 [*amyE*:: $P_{spank(hy)}$] were resuspended in GMD medium containing 1 mM IPTG and incubated at 37°C. Samples were taken at the indicated times. Cell membranes were stained with FM4-64. Cells or cell chains with one or more visible septa were scored as having divided. At least 125 germinated cells were counted for each sample.

since *yneA*-overexpressing cells appeared to cease exponential growth at approximately the same time as vector control cells (see Fig. S1 in the supplemental material). To address whether YneA affects cell separation in addition to septum formation, we quantitated chain length in populations overexpressing *yneA*. Five hours after induction, well into stationary phase, the *yneA*-overexpressing strain contained a greater number of cells per chain than the vector control did (Fig. 3A). The majority of uninduced cells existed as single cells, with 19% of the ob-

served chains being pairs and only a small percentage (<2%) containing three or more cells (Fig. 3B). In contrast, the frequency of longer chains, of three or more cells, in *yneA*-overexpressing populations was much higher (approximately 28%). Therefore, it appears that YneA inhibits not only septum formation but also daughter cell separation.

We sought to confirm this effect by triggering cell separation via nutrient downshift. When *Bacillus* cells are shifted from rich to starvation medium, they are known to separate into

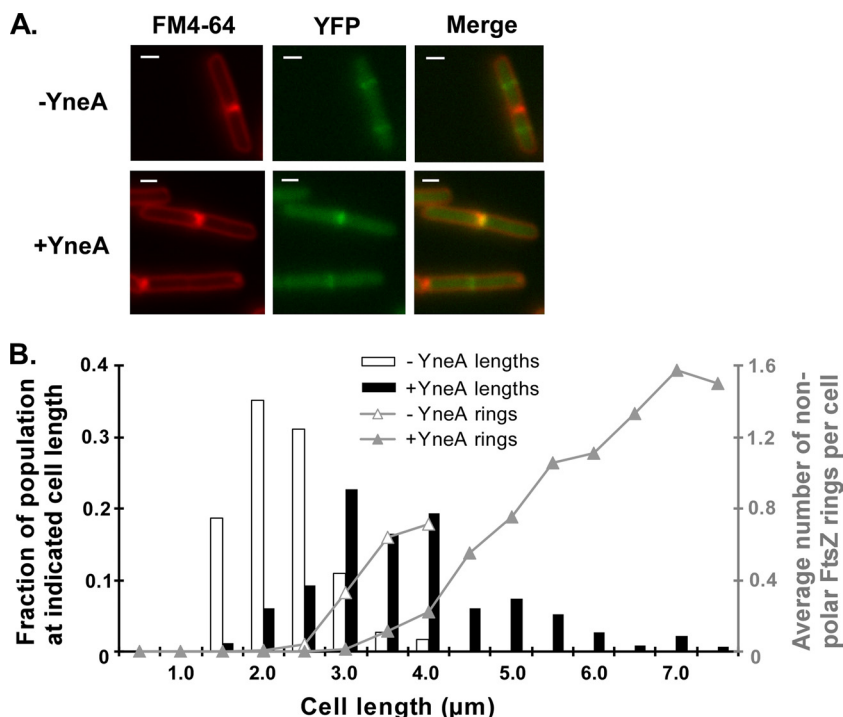


FIG. 2. YneA delays FtsZ ring formation. (A) FtsZ-YFP localization in cells expressing *yneA*. AM293 [*amyE*::*P_{xyf}-ftsZ-yfp thrC*::*P_{spank(hy)}-yneA*] was induced with 1 mM IPTG (+YneA) and 0.5% xylose. IPTG was omitted in one culture (-YneA). One hour after induction, cells were stained with FM4-64 and visualized. Bars, 1 μm. (B) YneA delays FtsZ ring assembly. Cell lengths were measured as described for Fig. 1C and were plotted with the length on the *x* axis and the fraction of the population at each length on the left *y* axis (bars). Fluorescent bands seen in the YFP channel that were not associated with completed septa or cell poles were scored as nonpolar FtsZ rings. The average number of these FtsZ rings per cell at each length was plotted on the right *y* axis (lines). More than 300 cells from each sample were measured. Of the >200 total FtsZ rings counted in each sample, between 15% (-YneA) and 37% (+YneA) were nonpolar. This experiment is representative of two independent trials.

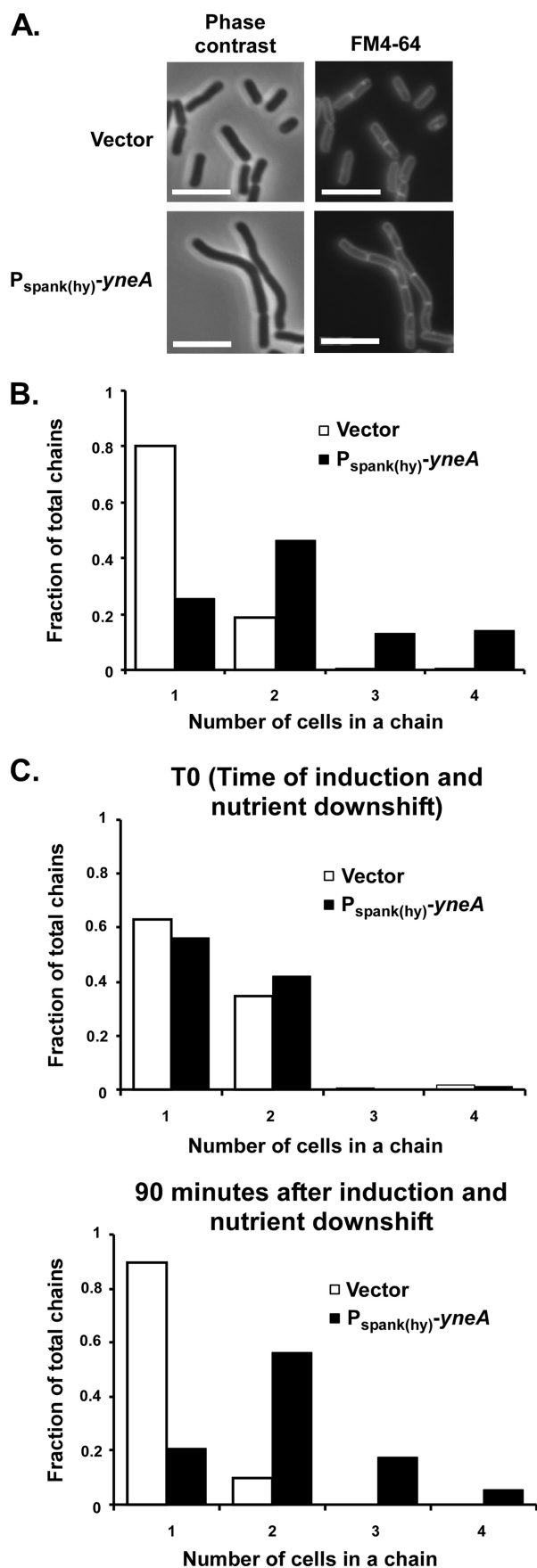
single cells as they enter the sporulation pathway (19). In order to test whether YneA can prevent cell separation under these conditions, we grew strains to exponential phase in rich CH medium and then resuspended the cultures in minimal SM medium with IPTG. At the time of resuspension (T₀), a significant proportion of cells (35 to 43%) formed chains of two or more (Fig. 3C). Ninety minutes following nutrient downshift and induction of the *yneA*-overexpressing strain, almost all vector control chains had separated into single cells, with only 10% remaining in pairs. In contrast, *yneA*-overexpressing cells existed in chains despite the shift to nutrient-limiting conditions, with comparatively few (20%) separating into single cells. In fact, there was an increase in higher-order chains of 3 or more cells (23%). Based on these experiments, in which *yneA*-overexpressing cells failed to separate even when cell separation was induced, YneA activity may have a direct effect on a late stage of division occurring after septation. However, we cannot rule out the possibility that delayed septation also contributes indirectly to the cell separation defect seen in *yneA*-overexpressing cells.

Cells rapidly resume division after *yneA* expression is shut off. From our analysis, it appears that YneA delays, rather than permanently blocks, cell division. Furthermore, to avoid a loss in viability, cells must have a mechanism for shutting off YneA activity, allowing the resumption of growth after DNA damage has been repaired. We examined the response of cells to transcriptional shutoff. In our IPTG-induced *yneA* overexpression

system, we mimicked the effect of shutting off the SOS response by resuspending *yneA*-overexpressing cells in fresh medium without inducer. Zero, 20, 40, and 60 min following resuspension, cell lengths were measured. Cells resumed division rapidly after *yneA* expression was shut off (Fig. 4). Within the first 20 min in the absence of inducer, cells that had previously been overexpressing *yneA* (+IPTG, -IPTG) underwent a great reduction in length, to sizes closer to that of uninduced control cells (-IPTG). On the other hand, *yneA*-overexpressing cells that were resuspended in medium containing inducer (+IPTG) remained relatively long in the 60 min following resuspension. These data are consistent with the idea that cells must be able to rapidly resume division once DNA damage is cleared.

YneA is rapidly cleaved and secreted into the medium. While *yneA* expression is controlled by the SOS response, posttranslational regulation of the YneA protein is not well understood. The predicted domains of YneA, based on sequence, are shown in Fig. 5A. Sequence analysis suggests that YneA is secreted. Using SignalP trained on Gram-positive bacteria (5; <http://www.cbs.dtu.dk/services/SignalP/>), a signal peptide was predicted with 99% probability, with cleavage between residues G31 and Q32. A LysM peptidoglycan domain makes up the majority of the C terminus of YneA (Pfam database [<http://www.sanger.ac.uk/Software/Pfam/>]).

We were unable to obtain useful antibodies against YneA, so we monitored export by using PhoA fused to the C terminus



of YneA. Assays of PhoA activity on indicator plates and in liquid culture confirmed that YneA is exported, and based on plate growth and morphology, YneA-PhoA is partially functional (data not shown). Since proteins translocated across the membrane may remain linked to the membrane, associate with the cell wall, or be released into the surrounding medium (12, 53), we wanted to determine where the YneA protein localized. We separated cells expressing *yneA-phoA* into cell-associated, wall-associated, and secreted fractions. Because of the presence of a LysM peptidoglycan binding domain in the exported C terminus, we expected that YneA would interact with the cell wall; however, the resulting immunoblot indicated that the vast majority of YneA was secreted into the medium, with only a small amount visible in the wall-associated fraction (Fig. 5B). In contrast, LytE-PhoA, a well-characterized wall-binding protein containing three LysM repeats (40), was found in the wall-associated fraction but not in the secreted fraction. Some LytE-PhoA was also present in the cell-associated fraction, probably due to contaminating cell wall material or the presence of unprocessed LytE-PhoA in the cell prior to export. As expected, the cytosolic DnaA protein was detected only in the cell-associated fraction. Therefore, despite the presence of a LysM domain, YneA appears to bind the cell wall only transiently.

Several secretory pathways have been characterized, but the majority of exported proteins in *B. subtilis* are translocated via the Sec pathway (53). The signal peptide of YneA is typical of this class of proteins, although the predicted cleavage site in YneA diverges somewhat from the consensus. SecA, a key component of the translocation machinery, is required for export via the Sec pathway (41). Using a temperature-sensitive allele of *secA*, we confirmed that export of YneA is SecA dependent. No secreted YneA was detected on an immunoblot when cells were shifted to the nonpermissive temperature (Fig. 5C). As a control, we used a *secA*⁺ strain background to show that YneA-PhoA is stable and exported at 45°C. Thus, YneA is likely to be secreted through the SecA pathway, with subsequent cleavage of the signal peptide.

Based on the fractionation experiments described above, it is clear that the signal peptide of YneA is cleaved, thereby releasing large amounts of YneA into the medium. We used

FIG. 3. YneA inhibits cell separation. (A) Cells overexpressing *yneA* remain in chains after the onset of stationary phase. Images are from the same experiment as that described for Fig. 1C. Cells were stained with FM4-64 and DAPI and were visualized 5 h after induction of *yneA* with 1 mM IPTG (stationary phase). Bars, 5 μm. (B) Quantitation of cell chain lengths from the same experiment as that for panel A. Samples were taken 5 h after induction of *yneA*. The number of cells per chain was determined by comparing phase-contrast and FM4-64-stained images. At least 400 cells (>200 chains) were counted for each strain. This experiment is representative of two independent trials under essentially the same conditions. (C) AM62 (*amyE::cat*) and AM93 [*amyE::P_{spank(hy)}-yneA*] were grown overnight on LB agar, resuspended in T-base, diluted to an OD₆₀₀ of ~0.02 in CH (rich) medium, and grown at 37°C to exponential growth phase (OD₆₀₀ = 0.3 to 0.5). Cells were then resuspended in SM (minimal) medium containing 1 mM IPTG. Samples were taken at the time of resuspension (top graph) and 90 min after resuspension (bottom graph), and chain lengths were quantified as in panel B. This experiment is representative of two independent trials.

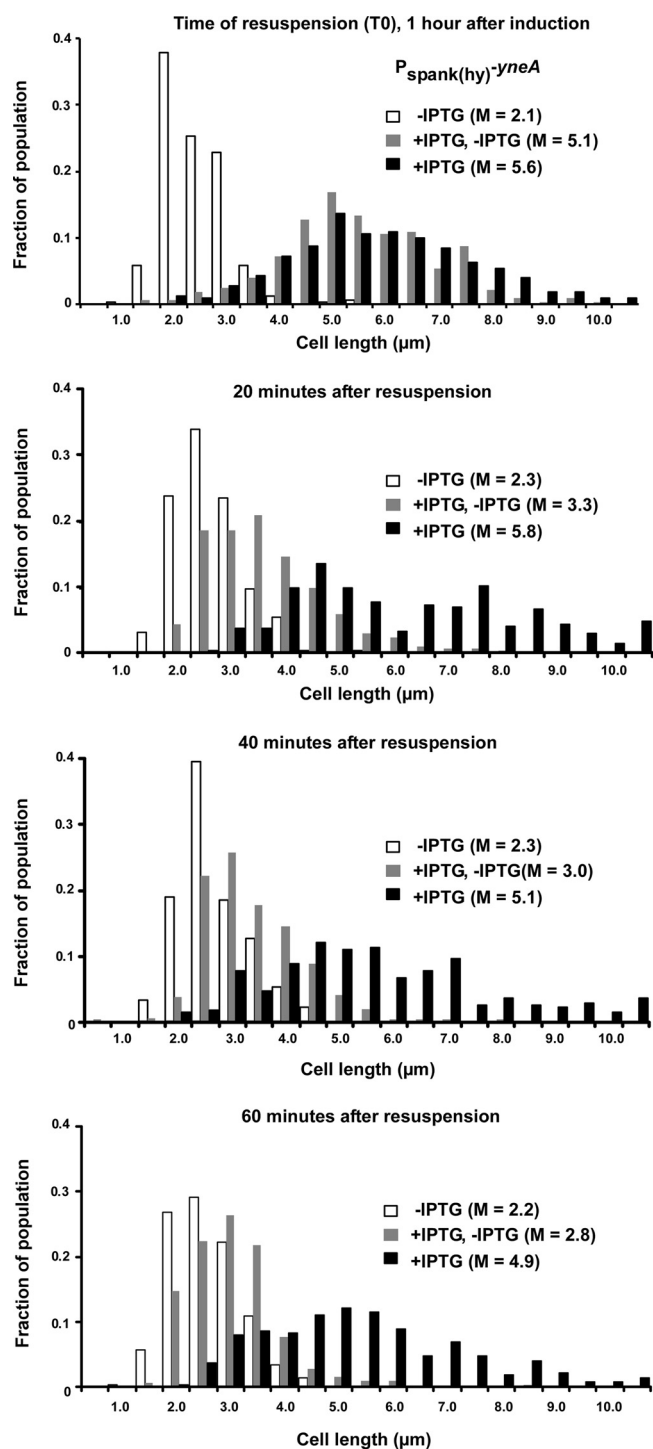


FIG. 4. Division resumes rapidly after *yneA* expression is shut off. AM69 [*amyE::P_{spank(hy)}-yneA*] was induced with 1 mM IPTG. IPTG was omitted in one culture throughout the experiment, as a control (-IPTG; white bars). One hour after induction, cells were centrifuged and resuspended in an equal volume of LB, with (+IPTG; black bars) or without (+IPTG, -IPTG; gray bars) 1 mM IPTG. Samples were taken 0, 20, 40, and 60 min after resuspension. Cells were stained and measured as described in the legend to Fig. 1C. This experiment is representative of two independent trials under essentially the same conditions.

epitope-tagged YneA in proteolysis rate experiments to determine the rate of signal peptide cleavage as well as to visualize any additional proteolytic processing of YneA. Analysis of cell-length distributions showed that the S-Flag-His10-tagged form of YneA is partially functional (see Fig. S2 in the supplemental material). Epitope-tagged YneA was overexpressed from an ectopic locus (*thrC*), and samples from the total culture were collected at short intervals following arrest of protein synthesis. Antibodies to the C-terminal S tag on YneA allowed us to examine the stability of YneA-S before and after signal peptide cleavage. Consistent with the fractionation experiments described above, full-length YneA-S was processed very rapidly and had a half-life of <5 min (Fig. 5D). In the wild-type background, we were unable to visualize the C-terminal portion of YneA that is released from the membrane upon signal peptide cleavage. Previous studies have shown that certain LysM-containing proteins are stabilized in strains lacking *wprA* and *epr*, two of the eight known genes encoding extracellular proteases in *B. subtilis* (61). We hypothesized that YneA might also be susceptible to these proteases. Indeed, when the proteolysis rate experiments were repeated with a strain lacking *wprA* and *epr*, a persistent band, presumed to be the signal peptide-cleaved C terminus of YneA, was evident (Fig. 5D). In support of this, the band migrated similarly to what would have been expected for the mature form of YneA-S on a 13.5% SDS-polyacrylamide gel. At least three additional, smaller products were also stabilized in the protease-deficient strain. These were likely the result of further degradation of the YneA C terminus by extracellular proteases. The stability of full-length YneA-S in the protease-deficient strain was similar to that of YneA-S in the wild-type background, consistent with the idea that full-length YneA is membrane bound and unlikely to be degraded by *wprA* and *epr*. Thus, two separate events may contribute to the posttranslational regulation of YneA, namely, signal peptide cleavage and, once it is released from the membrane, proteolysis of the C terminus.

Although so far the SOS response has not been found to regulate export, signal peptide cleavage, or extracellular protease activity, we wanted to ascertain that YneA induced with IPTG accurately mirrored the rate of proteolysis of SOS-induced YneA. We introduced YneA-S at the native *yneA* locus and induced the cells with 1 $\mu\text{g/ml}$ of mitomycin C. The stability of SOS-induced full-length YneA-S was similar to that of YneA-S induced with IPTG (Fig. 5E). We concluded that the cleavage and degradation of YneA are not regulated in response to DNA damage.

Residues affecting the stability and activity of YneA. Given the instability of full-length YneA, it seemed likely that signal peptide cleavage is one mechanism by which cells either rapidly activate YneA or shut it off. In order to determine which form of YneA is active, we identified mutations that either stabilized full-length YneA or increased the amount of cleaved YneA and then determined their effect on YneA's ability to inhibit division. First, we mutated the signal peptide cleavage site in YneA (SSGQ) to the consensus sequence AXAA (54). We predicted that this would increase the rate of signal peptide cleavage, thus creating more cleaved YneA product. In proteolysis rate experiments, YneA(ASAA)-S displayed a significantly larger amount of signal peptide-cleaved product than did wild-type YneA-S, which was visible on an immunoblot

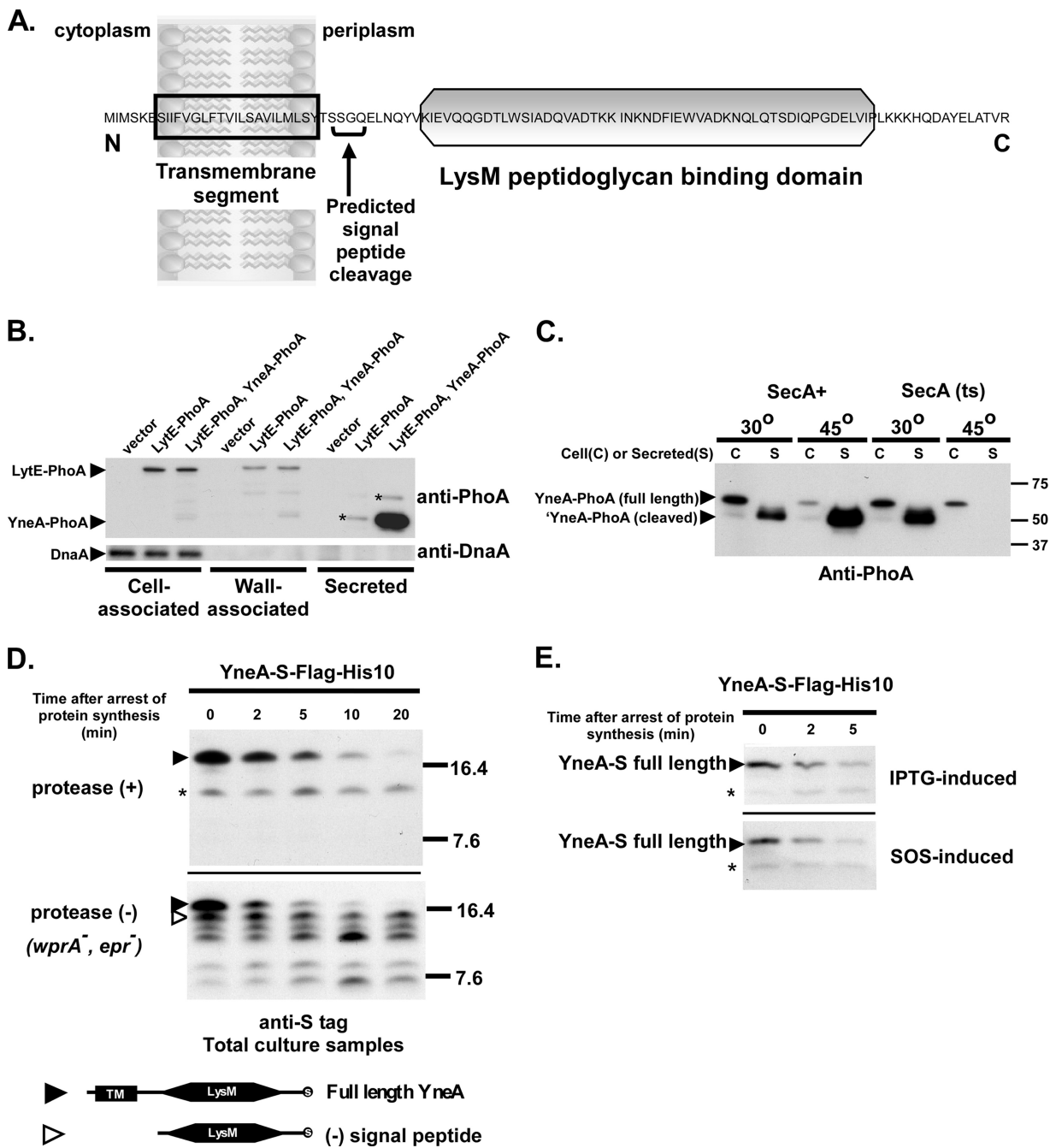


FIG. 5. YneA is rapidly cleaved and secreted into the medium. (A) Predicted domains of YneA. Predictions are based on sequence analysis using SignalP and Pfam. (B) YneA is secreted into the medium and does not associate strongly with the cell wall. Asterisks (*) indicate probable LytE-PhoA degradation products. AM206 [*thrC::P_{spank(hy)}*], AM218 [*lytE::lytE-phoA*], and AM222 [*lytE::lytE-phoA thrC::P_{spank(hy)}-yneA-phoA*] were grown in GYE minimal medium and induced with 1 mM IPTG. Two hours after induction, cultures were centrifuged and then separated into cell, wall, and secreted fractions as described in Materials and Methods. Samples were separated in a 10% SDS-polyacrylamide gel. Each lane contains 2 μg of cell fraction, 0.5 μg of wall fraction, or 0.5 μg of secreted fraction. Immunoblots were performed with either anti-PhoA antibody or anti-DnaA antibody. (C) YneA export is SecA dependent. AM98 [*thrC::P_{spank(hy)}-yneA-phoA*] and AM280 [*secA314(Ts) thrC::P_{spank(hy)}-yneA-phoA*] were incubated at either 30°C or 45°C in GYE medium containing 1 mM IPTG. After 1 h of induction, cultures were centrifuged and the secreted fraction prepared as described in Materials and Methods. Samples were separated in a 10% SDS-polyacrylamide gel. Each lane contains 2 μg of cell fraction or ~0.5 μg of secreted fraction. Immunoblots were performed with anti-PhoA antibody. (D) Full-length YneA is rapidly cleaved. Black arrowheads, full-length YneA-S-Flag-His10 (~16.9 kDa); open arrowheads, C-terminal portion of YneA-S-Flag-His10 lacking signal peptide (~13.5 kDa); asterisk, nonspecific band. AM199 [*thrC::P_{spank(hy)}-yneA-S-flag-his10*] and AM200 [*epr::tet wprA::kan thrC::P_{spank(hy)}-yneA-S-flag-his10*] were induced with 1 mM IPTG. After 1 h of induction, protein synthesis was inhibited with 200 μg ml⁻¹ chloramphenicol, and whole culture samples were removed at the indicated times after drug addition. S-tagged proteins were isolated as described in Materials and Methods and separated in a 13.8% SDS-polyacrylamide gel. Immunoblots were performed using diluted (1:5,000) anti-S primary antibody. (E) Induction of the SOS response does not affect the stability of YneA. AM199 [*thrC::P_{spank(hy)}-yneA-S-flag-his10*] and AM214 [*yneA::P_{spank(hy)}-yneA-S-flag-his10*] were induced with 1 mM IPTG and 1 μg ml⁻¹ mitomycin C, respectively. After 1 h of induction, protein synthesis was arrested, and samples were taken and treated as described for panel D.

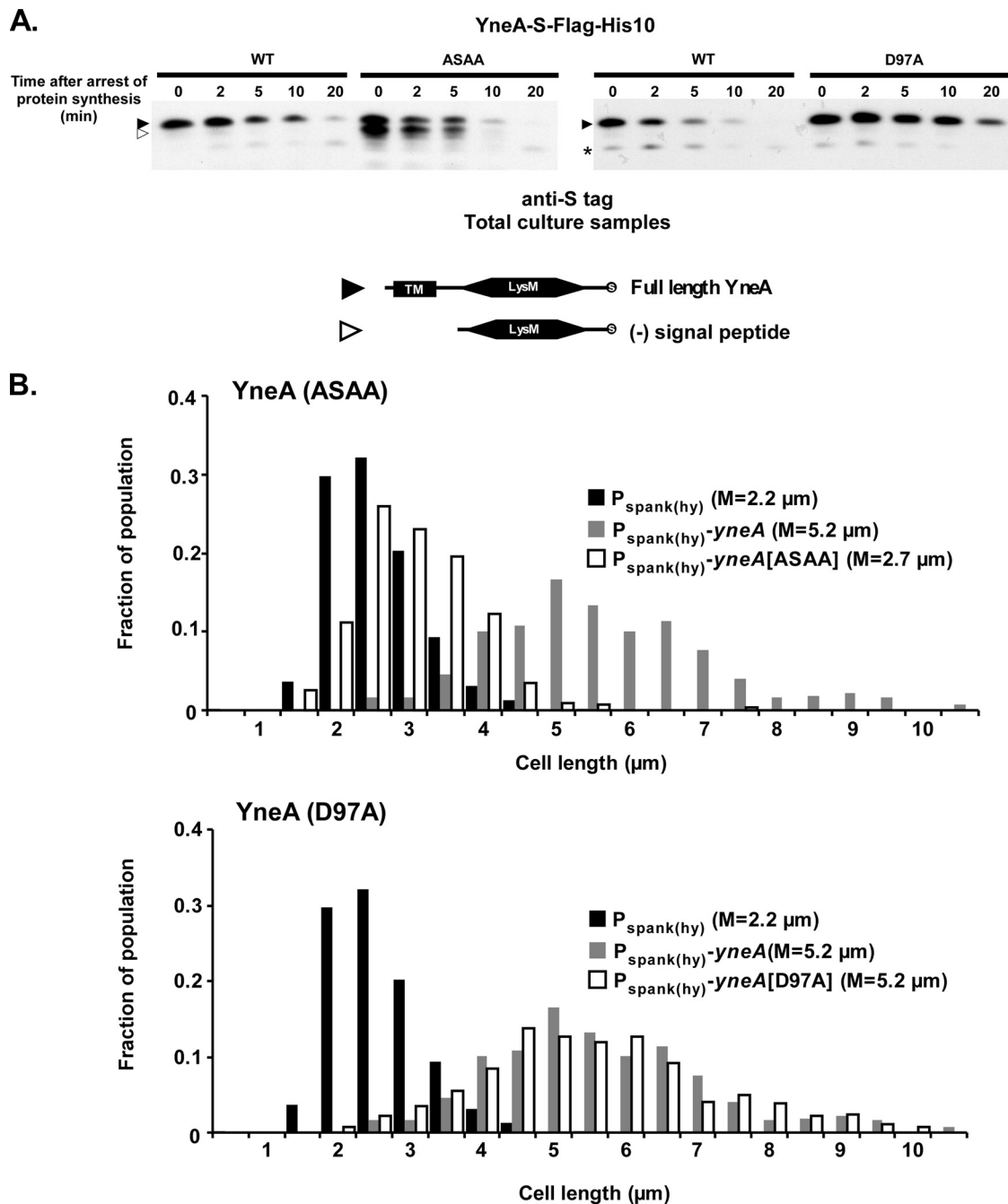


FIG. 6. Full-length YneA may be the active form. (A) ASAA and D97A mutations affect the stability of full-length and cleaved YneA. Black arrowheads, full-length YneA-S-Flag-His10; open arrowheads, C-terminal portion of YneA-S-Flag-His10 lacking the signal peptide; asterisk, nonspecific band. AM199 [*thrC*:: $P_{\text{spank}(\text{hy})}\text{-yneA-S-flag-his10}$], AM202 [*thrC*:: $P_{\text{spank}(\text{hy})}\text{-yneA(ASAA)-S-flag-his10}$], and AM228 [*thrC*:: $P_{\text{spank}(\text{hy})}\text{-yneA(D97A)-S-flag-his10}$] were grown and samples were prepared as described in the legend to Fig. 5D. Proteins were separated in a 13.8% SDS-polyacrylamide gel, and immunoblots were performed using diluted (1:5,000) anti-S primary antibody. (B) YneA(ASAA) is inactive, while YneA(D97A) remains active. AM69 [*amyE*:: $P_{\text{spank}(\text{hy})}\text{-yneA}$], AM70 [*amyE*:: $P_{\text{spank}(\text{hy})}$], AM133 [*amyE*:: $P_{\text{spank}(\text{hy})}\text{-yneA(ASAA)}$], and AM155 [*amyE*:: $P_{\text{spank}(\text{hy})}\text{-yneA(D97A)}$] were grown and induced, and cells were stained and measured as described in the legend to Fig. 1C. This experiment is representative of two independent trials.

even when the strain contained a full complement of extracellular proteases (Fig. 6A). We sought to make a mutation that would have the opposite effect on cleavage rate to that of ASAA. Previous studies suggested that inserting proline at the -1 or -3 site in the signal peptide cleavage site prevents cleavage (8, 51). However, mutating the YneA cleavage site to

PSPQ did not appear to stabilize full-length YneA (data not shown). It is possible that inserting prolines caused signal peptidase to recognize a different cleavage site nearby.

Fortuitously, while examining other regions of YneA, we identified a point mutation at the extreme C terminus (D97A) that appears to stabilize full-length YneA. YneA(D97A)-S was

cleaved at a lower rate than wild-type YneA-S, which was especially evident 10 and 20 min after the arrest of protein synthesis (Fig. 6A). This increased stability of YneA(D97A) relative to that of wild-type YneA was consistent over several independent experiments, although the half-life of YneA varied slightly from experiment to experiment. One explanation for this increased stability is that changing the D97 residue results in a conformational change or protein interaction that affects access to the signal peptide cleavage site region of YneA. This hypothesis seems plausible, as the ratio of full-length to cleaved product was increased in the YneA(ASAA, D97A)-S double mutant compared to that in the YneA(ASAA)-S mutant (data not shown).

We next wanted to correlate the prevalence of the full-length and cleaved forms of YneA with the ability to inhibit division. We overexpressed the *yneA(ASAA)* and *yneA(D97A)* mutants and quantified cell length as described above. The YneA(ASAA) strain displayed a median cell length similar to that of the vector control (median lengths of 2.7 μm and 2.2 μm , respectively), suggesting that increasing the amount of cleaved product inactivates YneA (Fig. 6B). It should be noted that YneA(ASAA) might have decreased activity if the mutation shifted cleavage away from the native site and inactivated the protein as a result. On the other hand, cells overexpressing *yneA(D97A)* were elongated to a similar extent to that for cells overexpressing wild-type *yneA* (both with median lengths of 5.2 μm). Therefore, stabilizing the full-length form of YneA does not reduce the ability of YneA to inhibit cell division. The behavior of the YneA(ASAA) and YneA(D97A) mutants suggests that YneA is active in the full-length form and that increasing the amount of cleaved YneA may reduce activity.

Since YneA(D97A) was cleaved more slowly than wild-type YneA, we asked if cells overexpressing *yneA(D97A)* would take longer to resume dividing after YneA expression was shut off. This was not the case, as we found that cells overexpressing wild-type *yneA* and *yneA(D97A)* resumed cell division with similar timing (data not shown). However, we note that the experimental conditions probably did not allow us to observe small changes in the amount of time required to resume division.

The largest distinguishing feature of YneA is the C-terminal LysM domain. LysM repeats are often found in proteins known to bind to the cell wall (13), although given our observation that YneA displays very little association with the wall (Fig. 5B), it is unclear whether the LysM domain is required for YneA function. A truncated version of YneA lacking the LysM domain and C-terminal tail was exported but was non-functional (data not shown). Based on that mutant, it appears that some portion of the C terminus is required for YneA activity.

The transmembrane region is required for YneA activity, independent of its role in protein export. The other identifiable feature of YneA is the transmembrane segment. We used alanine scanning mutagenesis to establish whether the transmembrane domain is required for YneA activity. Several of the resulting mutations abolished YneA function in a qualitative growth assay (Table 2). PhoA fusions were used to rule out export defects in these mutants. Strikingly, when the mutations were superimposed on a model of a transmembrane helix, inactivating mutations clustered on one face of the helix, while

TABLE 2. Residues in the transmembrane region are required for YneA activity

Strain	YneA Mutation	Growth inhibition ^a	Comments ^b
AM69	Wild type	+	
AM175, AM187	E6A	–	Exported
AM232, AM247	S7A	–	Exported
AM233, AM248	I8A	–	Exported
AM234	I9A	±	
AM235, AM250	F10A	–	Exported
AM236	V11A	–	
AM237, AM252	L13A	±	Exported
AM238, AM253	F14A	–	Exported
AM239, AM254	T15A	–	Exported; protein stability similar to that of the wild type
AM240	V16A	+	
AM241, AM255	I17A	±	Exported
AM242, AM256	S19A	±	Exported
AM243, AM257	V21A	–	Exported; full-length protein less stable than wild-type protein
AM244, AM258	I22A	–	Exported
AM245, AM259	L23A	–	Exported
AM220, AM260	L25A	–	Exported
AM221	S26A	+	

^a Strains were streaked onto LB agar and LB agar containing 1 mM IPTG and were incubated overnight at 30°C. The ability to form normally sized single colonies was assessed to determine YneA activity. +, inability to form single colonies on IPTG-containing plates, indistinguishable from phenotype of wild-type YneA; –, normal formation of single colonies, no growth defect on IPTG-containing plates compared to plates without IPTG; ±, intermediate growth, cases where only very small single colonies were able to form.

^b Protein export was determined by using YneA-PhoA fusions and assaying for blue colonies (indicating export of PhoA) on GYE-XP indicator plates. Strains used for PhoA assays are listed as the second strain in the first column of the table. Protein stability was assessed by performing proteolysis rate experiments, using the S-tagged form of YneA {AM261 [$P_{\text{spank(hy)}}$]-*yneA(T15A)*-S-flag-his10] and AM263 [$P_{\text{spank(hy)}}$]-*yneA(V21A)*-S-flag-his10] as described in Materials and Methods.

mutations that resulted in a partially or fully functional protein were grouped on the opposite face (Fig. 7A). We further characterized one of the inactivating mutations, T15A, and found that the rate of signal peptide cleavage for YneA(T15A)-S was similar to that for wild-type YneA-S (Fig. 7B). When cell lengths were quantified, cells overexpressing *yneA(T15A)* were less elongated than wild-type cells (median lengths of 3.3 μm and 5.2 μm , respectively), although still slightly longer overall than vector control cells (median length of 2.2 μm) (Fig. 7C). Thus, mutating the T15 residue reduces YneA activity, even though the mutant protein displays normal secretion and stability. It is possible that T15 is involved in a protein-protein interaction through the transmembrane helix that is required for YneA activity. An alignment of the *B. subtilis* YneA transmembrane region with orthologues from other Gram-positive bacterial species revealed that many of the inactivating mutations were in conserved residues (S7, I8, F10, T15, and L23) (Fig. 7D), supporting the idea that this face of the transmembrane region is important for function.

DISCUSSION

We have shown that YneA delays FtsZ ring formation and septation, as well as daughter cell separation following septation. YneA is an exported protein that transiently associates

with the cell wall. Unexpectedly, YneA appears to be active prior to signal peptide cleavage. YneA is rapidly proteolyzed, and cells quickly resume division after *yneA* expression is turned off. Furthermore, mutations in the transmembrane region of the YneA signal peptide inactivate YneA without affecting export or stability, suggesting that the transmembrane may dimerize or interact with other proteins. Taken together, these results suggest a novel mechanism for an inhibitor of cell division.

The cell length at which FtsZ rings are first observed in cells overexpressing *yneA* is longer than that for uninduced cells, suggesting that YneA may delay FtsZ ring assembly (Fig. 2). This may account for the delay in septation that we observed (Fig. 1), or YneA might also delay a step of septum assembly after FtsZ ring formation. Attempts to determine if YneA localizes to division sites by use of fluorescent fusion proteins have so far been unsuccessful. In addition, YneA also delays daughter cell separation following division (Fig. 3), which is consistent with the model that YneA influences cell wall remodeling during cytokinesis. In *B. subtilis*, cell separation is promoted by the LytC, LytD, LytE, LytF, LytG, and CwlS autolysins, several of which contain LysM domain repeats (23, 29, 50). LytC and LytD are also involved in other processes of cell wall turnover, cell elongation, and peptidoglycan remodeling that are important during cell division (6). Interference of these autolysins by YneA could explain the cell separation defect seen in *yneA*-overexpressing cells. In this model, disruption of autolytic activity could hinder peptidoglycan remodeling, which in turn might also delay septum formation.

YneA is smaller than the other SOS-induced cell division inhibitors that have been identified in Gram-positive bacteria, such as *M. tuberculosis* Rv2719c and *C. glutamicum* DivS (11, 14, 45). YneA consists only of the extracellular LysM domain, a short C-terminal sequence, and the signal peptide. Due to the presence of the LysM domain, we expected YneA to localize to the cell wall, with localization possibly needed to affect peptidoglycan remodeling. Instead, we determined that the vast majority of YneA was released into the surrounding medium after signal peptide cleavage (Fig. 5). It should be noted that peptidoglycan binding proteins often contain several LysM repeats, as opposed to the single LysM domain seen in YneA (13, 23). Our mutational analysis nevertheless suggests that the LysM domain and C-terminal tail are required for YneA function. It is possible that weak association of the single LysM domain of YneA with the cell wall modulates YneA activity, allowing cells to delay division transiently.

YneA is rapidly degraded and cells quickly resume division after transcription of *yneA* is shut off (Fig. 4 and 5). Unlike Rv2719c and DivS, which are integral membrane proteins, YneA contains a putative signal peptide cleavage site. Starting at the -3 position relative to the cleavage site, the predicted cleavage site sequence in YneA is SSGQ, which differs slightly from the consensus (AXAA, with the +1 site tolerating most residues, except for cysteine and proline [53, 54]). We were unable to isolate enough cleaved YneA protein to determine the exact site of cleavage; therefore, cleavage may actually occur at another site nearby. Our mutational analysis indicated that YneA may be active as a full-length protein: stabilizing the full-length form of YneA [YneA(D97A)] did not interfere with the ability of YneA to inhibit division, while increasing the

amount of cleaved YneA [YneA(ASAA)] decreased activity (Fig. 6). This is in contrast to many exported proteins that are inactive until released from the membrane by signal peptide cleavage. Full-length YneA-S had a half-life of <5 min (Fig. 5), although it is possible that the S tag affected the proteolysis rate. Five minutes, though rapid, is not as fast as the processing of certain secreted proteins with consensus cleavage sites (7, 55). Thus, the nonconsensus cleavage site of YneA may serve as a way to slow the action of signal peptidases, allowing full-length YneA to function. The fact that cleavage still occurred rather efficiently supports the role of YneA as a temporary inhibitor of division.

In addition to signal peptide cleavage, YneA is quickly degraded by extracellular proteases. Previous studies have implicated *epr* and *wprA* in the proteolysis of LysM-containing proteins (61), and we determined that this was also the case for YneA (Fig. 5). However, many of the eight known extracellular proteases in *B. subtilis* may be functionally redundant (1), so it is likely that there are other proteases that can degrade YneA after it has been released from the membrane. The proteolysis of YneA—signal peptide cleavage and degradation by extracellular proteases—appears to be constitutive. The rate of proteolysis was not affected by DNA damage or induction of the SOS response. Thus, the regulation of YneA follows the paradigm of some other checkpoint proteins, such as SfiA and Sda (an inhibitor of the sporulation cell cycle in *B. subtilis*), which are regulated at the level of transcription but are constitutively degraded (25, 43, 49). It should be noted that both signal peptide cleavage and C-terminal degradation by extracellular proteases may play a role in negatively regulating YneA activity, and our evidence does not clearly delineate which event is the rate-limiting step for shutting off YneA.

Surprisingly, mutations in the transmembrane region of the YneA signal peptide inactivated YneA without affecting protein export or stability (Fig. 7). This suggests that the transmembrane segment may interact with other proteins, homodimerizing, oligomerizing, or perhaps interacting directly with the target of YneA. Single-pass transmembrane domains have been shown to dimerize or oligomerize in a protein-specific manner (37, 46, 56). In some cases, protein-protein interactions in the membrane can promote or inhibit activity (see the discussion of divisome proteins below). A direct role for the transmembrane region in the inhibition of cell division by YneA is consistent with the model that full-length YneA is the active form. This does not preclude a role for the LysM domain, which might be needed, for example, to position YneA in the membrane or to localize YneA to sites of peptidoglycan synthesis.

Components of the *B. subtilis* divisome are attractive candidates for proteins that may interact with YneA via the transmembrane region. These single-spanning integral membrane proteins include DivIB, DivIC, PBP2b, and FtsL and assemble interdependently after FtsZ at division sites (reviewed in references 20 and 24). DivIB, DivIC, and FtsL interact to form a complex that is required for recruiting PBP2b and promoting septum formation (16, 18). Depleting DivIB or FtsL affects the stability of other proteins in the complex and can inhibit division (18). The transmembrane domain of DivIB is sufficient to localize the protein to the mid-cell, and previous studies have speculated that DivIB and FtsL interact through their trans-

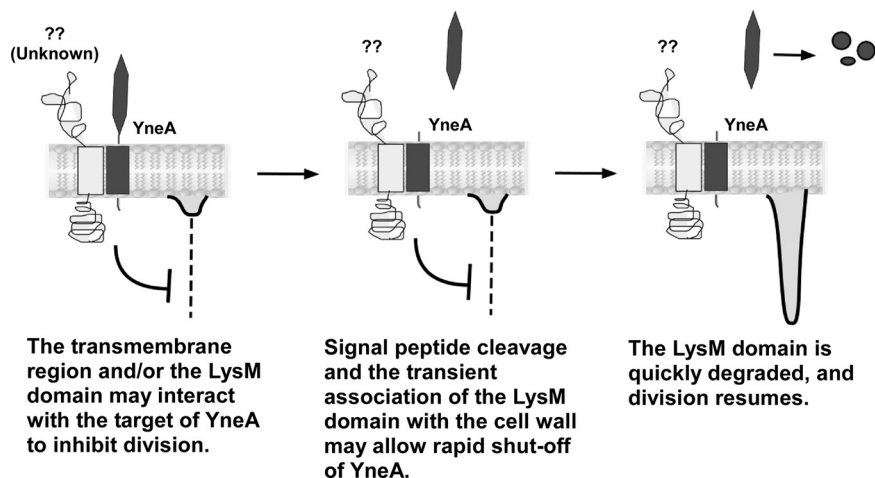


FIG. 8. Proposed model for YneA activity.

membrane domains (60). We have observed that a *divIB* mutation suppresses the growth defects caused by overexpressing *yneA* (unpublished data). One possibility is that YneA targets DivIB or another component of the divisome, thus disrupting or destabilizing the complex and preventing division. Depletion of PBP2b, one of a large family of penicillin-binding proteins (PBPs), results in cell elongation and aborted septal cross-wall formation (17). Therefore, it is possible that the cell separation defect we observed in *yneA*-overexpressing cells was due to defective PBP2b activity. Further study will be needed to determine if YneA interacts with the divisome, PBPs, or autolysins and whether targeting these proteins affects FtsZ ring assembly or stability.

We present one possible model for the regulation of YneA that is consistent with our data (Fig. 8). YneA interacts with another protein via the transmembrane region, resulting in inhibition of division (left panel). The LysM domain may also be involved in this protein-protein interaction, or it may help to localize YneA by transiently binding peptidoglycan. Signal peptide cleavage releases the LysM-containing C terminus into the medium (middle panel). The C-terminal portion of YneA is degraded by extracellular proteases (right panel). These constitutive proteolytic events may contribute to the rapid resumption of cell division following downregulation of *yneA* expression. This model represents a novel mechanism for an SOS-induced inhibitor of division and serves as a framework to guide future investigations regarding targets of YneA.

ACKNOWLEDGMENTS

We thank Peter Lewis, David Rudner, Junichi Sekiguchi, and Kunio Yamane for providing strains and plasmids, Steve Biller in the Burkholder lab for plasmid pSB243, and members of the Burkholder lab for helpful discussions.

A.H.M. was supported in part by an NIH predoctoral training grant (5T32GM007276). This work was supported by the National Science Foundation (award ID 0744872).

REFERENCES

- Antelmann, H., H. Yamamoto, J. Sekiguchi, and M. Hecker. 2002. Stabilization of cell wall proteins in *Bacillus subtilis*: a proteomic approach. *Proteomics* **2**:591–602.
- Au, N., E. Kuester-Schoeck, V. Mandava, L. E. Bothwell, S. P. Canny, K. Chachu, S. A. Colavito, S. N. Fuller, E. S. Groban, L. A. Hensley, T. C. O'Brien, A. Shah, J. T. Tierney, L. L. Tomm, T. M. O'Gara, A. I. Goranov, A. D. Grossman, and C. M. Lovett. 2005. Genetic composition of the *Bacillus subtilis* SOS system. *J. Bacteriol.* **187**:7655–7666.
- Autret, S., A. Levine, I. B. Holland, and S. J. Seror. 1997. Cell cycle checkpoints in bacteria. *Biochimie* **79**:549–554.
- Bateman, A., and M. Bycroft. 2000. The structure of a LysM domain from *E. coli* membrane-bound lytic murein transglycosylase D (MltD). *J. Mol. Biol.* **299**:1113–1119.
- Bendtsen, J. D., H. Nielsen, G. von Heijne, and S. Brunak. 2004. Improved prediction of signal peptides: SignalP 3.0. *J. Mol. Biol.* **340**:783–795.
- Blackman, S. A., T. J. Smith, and S. J. Foster. 1998. The role of autolysins during vegetative growth of *Bacillus subtilis* 168. *Microbiology* **144**:73–82.
- Bolhuis, A., H. Tjalsma, H. E. Smith, A. de Jong, R. Meima, G. Venema, S. Bron, and J. M. van Dijk. 1999. Evaluation of bottlenecks in the late stages of protein secretion in *Bacillus subtilis*. *Appl. Environ. Microbiol.* **65**:2934–2941.
- Borchert, T. V., and V. Nagarajan. 1991. Effect of signal sequence alterations on export of levansucrase in *Bacillus subtilis*. *J. Bacteriol.* **173**:276–282.
- Brehm, S. P., S. P. Staal, and J. A. Hoch. 1973. Phenotypes of pleiotropic sporulation mutants of *Bacillus subtilis*. *J. Bacteriol.* **115**:1063–1070.
- Bridges, B. A. 1995. Are there DNA damage checkpoints in *E. coli*? *Bioessays* **17**:63–70.
- Brooks, P. C., L. F. Dawson, L. Rand, and E. O. Davis. 2006. The mycobacterium-specific gene Rv2719c is DNA damage inducible independently of RecA. *J. Bacteriol.* **188**:6034–6038.
- Buist, G., A. N. Ridder, J. Kok, and O. P. Kuipers. 2006. Different subcellular locations of secretome components of Gram-positive bacteria. *Microbiology* **152**:2867–2874.
- Buist, G., A. Steen, J. Kok, and O. P. Kuipers. 2008. LysM, a widely distributed protein motif for binding to (peptido)glycans. *Mol. Microbiol.* **68**:838–847.
- Chauhan, A., H. Lofton, E. Maloney, J. Moore, M. Fol, M. V. Madiraju, and M. Rajagopalan. 2006. Interference of *Mycobacterium tuberculosis* cell division by Rv2719c, a cell wall hydrolase. *Mol. Microbiol.* **62**:132–147.
- Cordell, S. C., E. J. Robinson, and J. Lowe. 2003. Crystal structure of the SOS cell division inhibitor SulA and in complex with FtsZ. *Proc. Natl. Acad. Sci. U. S. A.* **100**:7889–7894.
- Daniel, R. A., and J. Errington. 2000. Intrinsic instability of the essential cell division protein FtsL of *Bacillus subtilis* and a role for DivIB protein in FtsL turnover. *Mol. Microbiol.* **36**:278–289.
- Daniel, R. A., E. J. Harry, and J. Errington. 2000. Role of penicillin-binding protein PBP 2B in assembly and functioning of the division machinery of *Bacillus subtilis*. *Mol. Microbiol.* **35**:299–311.
- Daniel, R. A., M. F. Noirot-Gros, P. Noirot, and J. Errington. 2006. Multiple interactions between the transmembrane division proteins of *Bacillus subtilis* and the role of FtsL instability in divisome assembly. *J. Bacteriol.* **188**:7396–7404.
- Dunn, G., and J. Mandelstam. 1977. Cell polarity in *Bacillus subtilis*: effect of growth conditions on spore positions in sister cells. *J. Gen. Microbiol.* **103**:201–205.
- Errington, J., R. A. Daniel, and D. J. Scheffers. 2003. Cytokinesis in bacteria. *Microbiol. Mol. Biol. Rev.* **67**:52–65.
- Feucht, A., and P. J. Lewis. 2001. Improved plasmid vectors for the production of multiple fluorescent protein fusions in *Bacillus subtilis*. *Gene* **264**:289–297.

22. **Friedberg, E. C.** 2006. DNA repair and mutagenesis, 2nd ed. ASM Press, Washington, DC.
23. **Fukushima, T., A. Afkham, S. Kurosawa, T. Tanabe, H. Yamamoto, and J. Sekiguchi.** 2006. A new D_{1L} -endopeptidase gene product, YojL (renamed Cw1S), plays a role in cell separation with LytE and LytF in *Bacillus subtilis*. *J. Bacteriol.* **188**:5541–5550.
24. **Goehring, N. W., and J. Beckwith.** 2005. Diverse paths to midcell: assembly of the bacterial cell division machinery. *Curr. Biol.* **15**:R514–R526.
25. **Gottesman, S.** 2003. Proteolysis in bacterial regulatory circuits. *Annu. Rev. Cell Dev. Biol.* **19**:565–587.
26. **Harry, E. J., J. Rodwell, and R. G. Wake.** 1999. Co-ordinating DNA replication with cell division in bacteria: a link between the early stages of a round of replication and mid-cell Z ring assembly. *Mol. Microbiol.* **33**:33–40.
27. **Harwood, C. R., and S. M. Cutting (ed.).** 1990. Molecular biological methods for *Bacillus*. John Wiley & Sons, Chichester, United Kingdom.
28. **Hirose, I., K. Sano, I. Shioda, M. Kumano, K. Nakamura, and K. Yamane.** 2000. Proteome analysis of *Bacillus subtilis* extracellular proteins: a two-dimensional protein electrophoretic study. *Microbiology* **146**:65–75.
29. **Horsburgh, G. J., A. Atrih, M. P. Williamson, and S. J. Foster.** 2003. LytG of *Bacillus subtilis* is a novel peptidoglycan hydrolase: the major active glucosaminidase. *Biochemistry* **42**:257–264.
30. **Huang, J., C. Cao, and J. Lutkenhaus.** 1996. Interaction between FtsZ and inhibitors of cell division. *J. Bacteriol.* **178**:5080–5085.
31. **Huisman, O., and R. D'Ari.** 1983. Effect of suppressors of SOS-mediated filamentation on *sfIA* operon expression in *Escherichia coli*. *J. Bacteriol.* **153**:169–175.
32. **Huisman, O., R. D'Ari, and S. Gottesman.** 1984. Cell-division control in *Escherichia coli*: specific induction of the SOS function SfiA protein is sufficient to block septation. *Proc. Natl. Acad. Sci. U. S. A.* **81**:4490–4494.
33. **Janion, C.** 2008. Inducible SOS response system of DNA repair and mutagenesis in *Escherichia coli*. *Int. J. Biol. Sci.* **4**:338–344.
34. **Janion, C.** 2001. Some aspects of the SOS response system—a critical survey. *Acta Biochim. Pol.* **48**:599–610.
35. **Kawai, Y., S. Moriya, and N. Ogasawara.** 2003. Identification of a protein, YneA, responsible for cell division suppression during the SOS response in *Bacillus subtilis*. *Mol. Microbiol.* **47**:1113–1122.
36. **Kelley, W. L.** 2006. Lex marks the spot: the virulent side of SOS and a closer look at the LexA regulon. *Mol. Microbiol.* **62**:1228–1238.
37. **Lemmon, M. A., and D. M. Engelman.** 1994. Specificity and promiscuity in membrane helix interactions. *FEBS Lett.* **346**:17–20.
38. **Little, J. W., and D. W. Mount.** 1982. The SOS regulatory system of *Escherichia coli*. *Cell* **29**:11–22.
39. **Love, P. E., and R. E. Yasbin.** 1986. Induction of the *Bacillus subtilis* SOS-like response by *Escherichia coli* RecA protein. *Proc. Natl. Acad. Sci. U. S. A.* **83**:5204–5208.
40. **Margot, P., M. Wahlen, A. Gholamhoseinian, P. Piggot, and D. Karamata.** 1998. The *lytE* gene of *Bacillus subtilis* 168 encodes a cell wall hydrolase. *J. Bacteriol.* **180**:749–752.
41. **McNicholas, P., T. Rajapandi, and D. Oliver.** 1995. SecA proteins of *Bacillus subtilis* and *Escherichia coli* possess homologous amino-terminal ATP-binding domains regulating integration into the plasma membrane. *J. Bacteriol.* **177**:7231–7237.
42. **Miller, J. H.** 1972. Experiments in molecular genetics. Cold Spring Harbor Laboratory, Cold Spring Harbor, NY.
43. **Mizusawa, S., and S. Gottesman.** 1983. Protein degradation in *Escherichia coli*: the *lon* gene controls the stability of SulA protein. *Proc. Natl. Acad. Sci. U. S. A.* **80**:358–362.
44. **Msadek, T., V. Dartois, F. Kunst, M. L. Herbaud, F. Denizot, and G. Rapoport.** 1998. ClpP of *Bacillus subtilis* is required for competence development, motility, degradative enzyme synthesis, growth at high temperature and sporulation. *Mol. Microbiol.* **27**:899–914.
45. **Ogino, H., H. Teramoto, M. Inui, and H. Yukawa.** 2008. DivS, a novel SOS-inducible cell-division suppressor in *Corynebacterium glutamicum*. *Mol. Microbiol.* **67**:597–608.
46. **Ottemann, K. M., and J. J. Mekalanos.** 1996. The ToxR protein of *Vibrio cholerae* forms homodimers and heterodimers. *J. Bacteriol.* **178**:156–162.
47. **Payne, M. S., and E. N. Jackson.** 1991. Use of alkaline phosphatase fusions to study protein secretion in *Bacillus subtilis*. *J. Bacteriol.* **173**:2278–2282.
48. **Radman, M.** 1975. SOS repair hypothesis: phenomenology of an inducible DNA repair which is accompanied by mutagenesis. *Basic Life Sci.* **5A**:355–367.
49. **Ruvolo, M. V., K. E. Mach, and W. F. Burkholder.** 2006. Proteolysis of the replication checkpoint protein Sda is necessary for the efficient initiation of sporulation after transient replication stress in *Bacillus subtilis*. *Mol. Microbiol.* **60**:1490–1508.
50. **Smith, T. J., S. A. Blackman, and S. J. Foster.** 2000. Autolysins of *Bacillus subtilis*: multiple enzymes with multiple functions. *Microbiology* **146**:249–262.
51. **Stephenson, S., C. Mueller, M. Jiang, and M. Perego.** 2003. Molecular analysis of Phr peptide processing in *Bacillus subtilis*. *J. Bacteriol.* **185**:4861–4871.
52. **Sutton, M. D., B. T. Smith, V. G. Godoy, and G. C. Walker.** 2000. The SOS response: recent insights into umuDC-dependent mutagenesis and DNA damage tolerance. *Annu. Rev. Genet.* **34**:479–497.
53. **Tjalsma, H., H. Antelmann, J. D. Jongbloed, P. G. Braun, E. Darmon, R. Dorenbos, J. Y. Dubois, H. Westers, G. Zanen, W. J. Quax, O. P. Kuipers, S. Bron, M. Hecker, and J. M. van Dijk.** 2004. Proteomics of protein secretion by *Bacillus subtilis*: separating the “secrets” of the secretome. *Microbiol. Mol. Biol. Rev.* **68**:207–233.
54. **Tjalsma, H., A. Bolhuis, J. D. Jongbloed, S. Bron, and J. M. van Dijk.** 2000. Signal peptide-dependent protein transport in *Bacillus subtilis*: a genome-based survey of the secretome. *Microbiol. Mol. Biol. Rev.* **64**:515–547.
55. **Tjalsma, H., M. A. Noback, S. Bron, G. Venema, K. Yamane, and J. M. van Dijk.** 1997. *Bacillus subtilis* contains four closely related type I signal peptidases with overlapping substrate specificities. Constitutive and temporally controlled expression of different *sip* genes. *J. Biol. Chem.* **272**:25983–25992.
56. **Toutain, C. M., D. J. Clarke, J. A. Leeds, J. Kuhn, J. Beckwith, I. B. Holland, and A. Jacq.** 2003. The transmembrane domain of the DnaJ-like protein DjaA is a dimerisation domain. *Mol. Genet. Genomics* **268**:761–770.
57. **Trusca, D., S. Scott, C. Thompson, and D. Bramhill.** 1998. Bacterial SOS checkpoint protein SulA inhibits polymerization of purified FtsZ cell division protein. *J. Bacteriol.* **180**:3946–3953.
58. **van der Veen, S., and T. Abee.** 2010. Dependence of continuous-flow biofilm formation by *Listeria monocytogenes* EGD-e on SOS response factor YneA. *Appl. Environ. Microbiol.* **76**:1992–1995.
59. **van der Veen, S., S. van Schalkwijk, D. Molenaar, W. M. de Vos, T. Abee, and M. H. Wells-Bennik.** 2010. The SOS response of *Listeria monocytogenes* is involved in stress resistance and mutagenesis. *Microbiology* **156**:374–384.
60. **Wadsworth, K. D., S. L. Rowland, E. J. Harry, and G. F. King.** 2008. The divisomal protein DivIB contains multiple epitopes that mediate its recruitment to incipient division sites. *Mol. Microbiol.* **67**:1143–1155.
61. **Yamamoto, H., S. Kurosawa, and J. Sekiguchi.** 2003. Localization of the vegetative cell wall hydrolases LytC, LytE, and LytF on the *Bacillus subtilis* cell surface and stability of these enzymes to cell wall-bound or extracellular proteases. *J. Bacteriol.* **185**:6666–6677.